JOURNAL OF SOLID STATE CHEMISTRY 113, 405–412 (1994)

Synthesis and Characterization of Some Iron Oxides by Sol-Gel Method

G. M. da Costa,[1,2] E. De Grave, P. M. A. de Bakker, and R. E. Vandenberghe

Department of Subatomic and Radiation Physics, Laboratory of Magnetism, University of Gent, B-9000, Gent, Belgium

Received October 7, 1993; in revised form February 15, 1994; accepted April 13, 1994

Several iron oxides and mixtures of iron oxides have been prepared by heating the product of a sol-gel reaction between iron(III) nitrate and ethylene glycol in different atmospheres and at different temperatures. The materials were characterized by Mössbauer spectroscopy, powder X-ray diffraction, and transmission electron microscopy. Ferrous iron was found to be present in an appreciable amount in the products of the sol-gel reaction, but its origin is not yet understood. Heating at 300°C in N_2 atmosphere, cooling in air to ambient temperature, and heating again at 300°C in static air produced single-phase maghemite with a mean crystallite diameter (MCD) of 18 nm. Well crystallized hematite (MCD = 110 nm) was obtained at 300°C in O_2 atmosphere. Mixtures of poorly crystallized maghemite and magnetite were observed to exhibit room-temperature Mössbauer spectra which closely resemble those reported for sodium-modified maghemite. A mixture of magnetite, wustite, and metallic iron was obtained by heating at 800°C in N_2 atmosphere.

INTRODUCTION

In recent years there has been an increasing interest in alternative methods for the production of iron oxides, in particular of hematite (α-Fe_2O_3) and magnetite (Fe_3O_4). So far the vast majority of these compounds have been prepared in hydrothermal conditions. By careful control of pH, temperature, concentration of the reactants, etc., it is possible to obtain pure compounds (1). On the other hand, some iron oxides are normally not obtained directly under these conditions, and so they have to be prepared by using a precursor. A notable example in that respect is maghemite (γ-Fe_2O_3), a ferrimagnet which is widely used as a magnetic recording medium. Its synthesis is usually carried out by oxidation of magnetite at temperatures not exceeding 300°C since at higher temperatures hematite is formed. This thermal instability of maghemite is a substantial disadvantage because it implies that the material cannot be annealed properly in order to minimize lattice defects or to ameliorate the grain growth.

Another shortcoming of the hydrothermal method for synthesis of iron oxides concerns the incorporation of foreign cations into the lattice. For instance, it has been suggested that Al-for-Fe substitution in maghemite is restricted to 10 at.% if the oxide is prepared from precursors that have been synthesized in hydrothermal conditions, whereas up to 66 at.% of substitution has been reported in the case of an organic precursor (2).

A very promising method for the synthesis of maghemite thin films was proposed by Takahashi *et al.* using a sol-gel reaction (3). Two years later Yamanobe *et al.* applied the same technique to obtain powders of what was claimed to be maghemite and sodium-substituted maghemite (4). However, the Mössbauer results presented in this latter paper for Na–maghemite seem to be quite different from most of the literature data for spinel compounds. The magnetic hyperfine fields at room temperature (RT) were quoted to be ≅425 and ≅485 kOe for ferric ions on tetrahedral (A) and octahedral (B) lattice sites, respectively. Such a large difference in fields is very uncommon for spinel ferrites (5). No details about the fitting procedures were given, nor were the values obtained for the other Mössbauer parameters.

In order to explore in greater detail the ability of the sol-gel method for the synthesis of maghemite, we have performed some experiments in addition to those described by Yamanobe *et al.* (4). The produced materials have been characterized by Mössbauer spectroscopy (MS), X-ray diffraction (XRD), and transmission electronic microscopy (TEM).

EXPERIMENTAL

Two samples of the precursor were synthesized as in (4), but without the addition of sodium ethylate. Fourteen grams of $Fe(NO_3)_3 \cdot 9H_2O$ (purity better than 99.0%, Merck) was dissolved in 55 g of ethylene glycol in a three-port glass flask and afterwards heated at 60°C for 2 hr in N_2 gas flow and under continuous stirring. The gel thus

[1] To whom correspondence should be addressed.

[2] On leave from Departamento de Química, Universidade Federal de Ouro Preto, Ouro Preto- MG, Brazil.

0022-4596/94 $6.00

obtained was transferred to a Petri dish and dried in air at 110°C during 24–36 hr. This sample is named ET8. The second sample (ET9) was prepared at 80°C under the same conditions. Iron oxides were obtained by subsequently heating the above materials at variable temperatures and atmospheres as specified below for ET9:

Sample	Conditions
ET92H3N	Sample ET9 heated at 300°C in N_2 gas flow and removed from the furnace after 2 hr
ET92H3A	Same as previous, but using O_2 gas instead of N_2
ET9D	Obtained by heating ET92H3N at 300°C in static air during 2 hr and cooled down outside the furnace
ET9H	Obtained as ET92H3N, but the sample was allowed to cool down inside the furnace under N_2 atmosphere
ET9I	Sample ET9H heated at 800°C during 2 hr in N_2 gas flow and cooled in the same manner as ET9H

An identical set of samples was prepared with ET8 as parent material.

Powder X-ray diffraction patterns were obtained using a Philips diffractometer with Co$K\alpha$ radiation and a graphite monochromator. The scannings were carried out at a speed of 1/4° min^{-1}. The data were collected in 2048 channels of a multichannel analyzer. The diffractograms were fitted with a sum of pseudo-Lorentzians, two for each peak in order to account for the $K_{\alpha 1}$ and $K_{\alpha 2}$ radiation. Mean crystallite diameters (MCD) were estimated from the full widths at half maximum (FWHM) using Scherrer's equation (6) with $K = 0.9$. Lattice parameters for the spinel phase were determined by the Nelson–Riley extrapolation method (6).

The morphology of the products was further examined with transmission electron microscopy.

Mössbauer spectra were collected with a time-mode spectrometer using a constant-acceleration drive and a triangular reference signal. All absorbers were prepared by mixing an amount of material with very pure carbon to achieve a homogeneous thickness of approximately 10 mg Fe/cm^2. The spectrometer was periodically calibrated using the spectrum of a well crystallized hematite absorber. Center shifts (δ) are quoted relative to metallic iron.

RESULTS AND DISCUSSION

X-ray diffraction patterns of both ET8 and ET9 in the region of 15–80° (2θ) consist of only one very broad peak around 27°. From its width the particle size is estimated to be less than 3 nm.

Mössbauer spectra of samples ET8 and ET9 at RT and 80 K are shown in Fig. 1. The presence of an appreciable amount of Fe^{2+} is evident. The spectra were fitted with two distributions of quadrupole splittings (ΔE_Q), and the resulting parameters are listed in Table 1. Sample ET8 contains slightly less Fe^{2+}, an effect that must be attributed to the lower temperature of synthesis since this was the only difference between the two preparations. Chemical analysis using the dichromate method yielded the following values for the iron contents (weight percent):

ET8: wt.% Fe^{2+} = 6.2 wt.% Fe_{total} = 28.2 Fe^{2+}/Fe^{3+} = 0.28

ET9: wt.% Fe^{2+} = 7.1 wt.% Fe_{total} = 28.9 Fe^{2+}/Fe^{3+} = 0.33

It is well known that the area S of a Mössbauer spectrum of a given iron species is to a good approximation proportional to the product $f \cdot n$, n being the number of the corresponding iron atoms and f their Mössbauer fraction. Recently, it has been shown that the f-factors for Fe^{2+} and Fe^{3+} ions in a given compound are not the same, and considering a large number of experimental data for various types of ferrous- and/or ferric-containing substances, it was suggested that the ratio $f_{Fe^{2+}}/f_{Fe^{3+}}$ is on the average approximately 0.9 (7). Based on this value, the Fe^{2+}/Fe^{3+} ratios, evaluated from the relative spectral areas RA of the ferrous and ferric quadrupole doublets (see Table 1), were found to be 0.26 and 0.31 for ET8 and ET9, respectively. These results are in excellent agreement with those from the chemical analyses.

The presence of ferrous ions in the precursor was also observed after the synthesis was carried out in an O_2 gas flow, but in this case the ratio Fe^{2+}/Fe^{3+} was lowered to 0.12, indicating that the presence of O_2 inhibits the formation of Fe^{2+} species, which is rather puzzling. In contrast, the amount of ferrous ions did not change significantly when the reaction was carried out for 5 hr instead of 2 hr. So far, the mechanism leading to the formation and the nature of this ferrous phase remain unclear.

The first attempts to obtain maghemite consisted of heating ET9 at 300°C under static air, as proposed by Yamanobe *et al.* (4), and subsequently in a stream of N_2 gas. Both products turned out to be almost exactly the same and are composed of black grains mixed with brown ones. The latter were observed to form as soon as the materials were removed from the furnace. Both phases are highly magnetic. The reason why similar products are obtained under these two different atmospheres is believed to be that, during heating under static air, the sample is actually subjected to a complex atmosphere originating from the decomposition of the organic part of the precursor and preventing complete oxidation of the

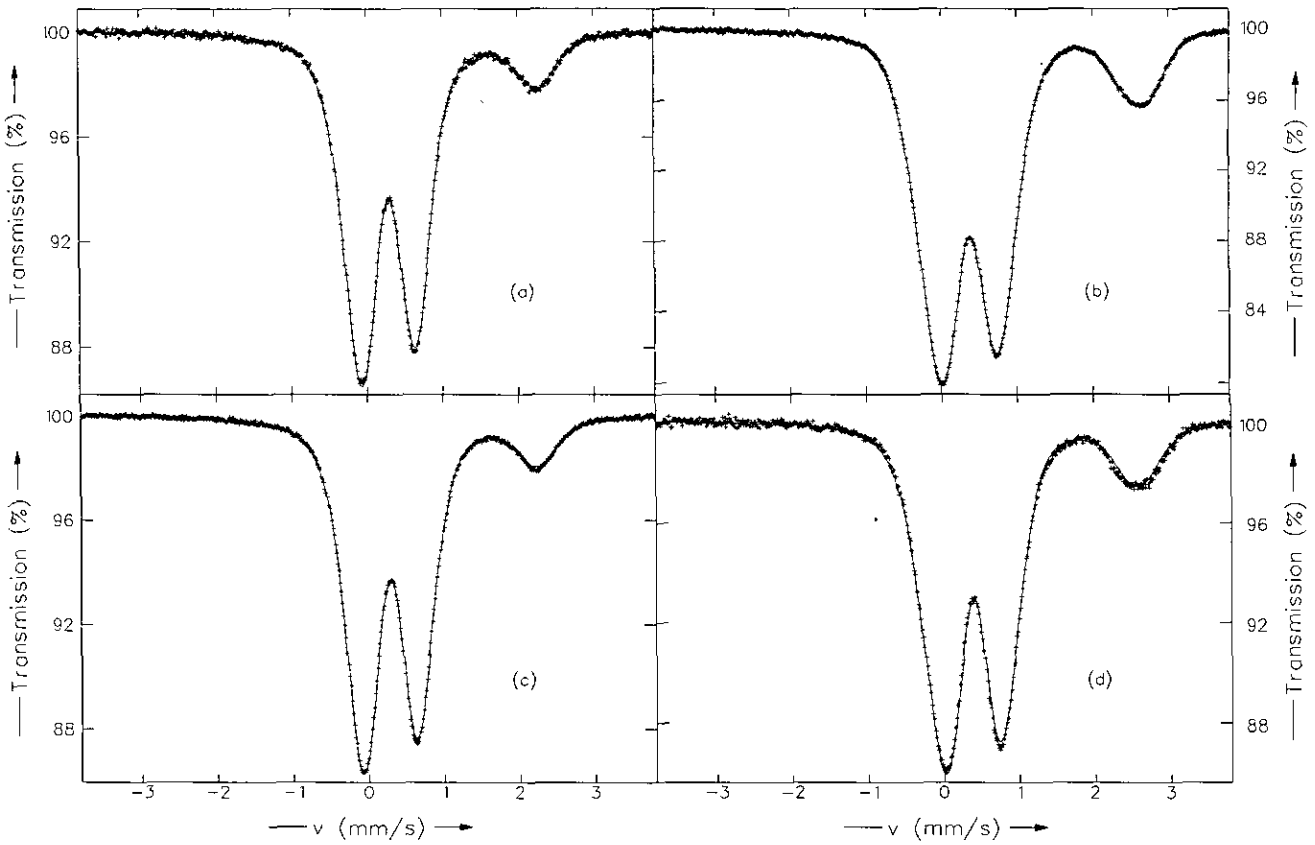

FIG. 1. Mössbauer spectra of the products of the sol-gel reaction: (a) ET9 at RT, (b) ET9 at 80 K, (c) ET8 at RT, and (d) ET8 at 80 K.

ferrous species. Only one sample, ET92H3N, will be retained for further discussions.

The XRD pattern of sample ET92H3N is shown in Fig. 2 (top). All diffraction lines (except those at ≅45 and ≅52° which are due to the Al sample holder) can be assigned to a spinel phase (i.e., γ-Fe_2O_3 and/or Fe_3O_4). The cubic lattice parameter of this spinel phase was calculated from the (220), (311), (400), (422), (333), and (440) reflections and is listed in Table 2, along with the calculated mean crystallite diameter. Magnetite above the Verwey-transition temperature ($T_V \cong 125$ K) and maghemite exhibit the same crystalline structure, and their XRD patterns are almost identical. It is therefore usually quite difficult to distinguish between the two oxides, especially if significant line broadening occurs as a result of small particle sizes, which is the case for ET92H3N. As Table 2 shows, the lattice parameter for this sample is between that for magnetite (0.8396 nm, JCPDS card #19.629) and that for maghemite (0.8350 nm, JCPDS card #4.755), and hence the sample could be a mixture of both, or an intermediate phase (partially oxidized magnetite).

TABLE 1
Mössbauer Parameters at RT and 80 K Derived from the Quadrupole-Distribution Fits for Samples ET9 and ET8

Sample	Temp.	ΔE_Q^b	ΔE_Q^c	ΔE_Q^{max}	$\overline{\Delta E_Q}$	δ	FWHM	RA
ET9	RT	1.5	3.5	2.47	2.42	1.12	0.46	22
		0	2.0	0.68	0.74	0.39	0.27	78
	80 K	1.5	4.0	2.86	2.80	1.24	0.38	26
		0	2.0	0.71	0.77	0.48	0.25	74
ET8	RT	1.5	3.5	2.47	2.43	1.11	0.45	19
		0	2.0	0.70	0.76	0.40	0.29	81
	80 K	1.5	4.0	3.05	2.91	1.28	0.36	18
		0	2.0	0.70	0.78	0.46	0.23	82

Note. ΔE_Q^b and ΔE_Q^c are the lower and upper limits for the distributions; ΔE_Q^{max} and $\overline{\Delta E_Q}$ are the maximum-probability and average values; δ is the center shift corresponding with the average quadrupole splitting. All values are given in mm/sec, except the relative area RA, which is given in %.

In an attempt to find some indication for the presence of magnetite in ET92H3N, its RT Mössbauer spectrum was fitted with a superposition of two model-independent distributions of hyperfine fields (H_{hf}), along with one distribution of quadrupole splittings. A linear correlation between the hyperfine fields and center shifts was imposed, but it was observed that this correlation is significant for the low-field component only. As Fig. 3a shows, the

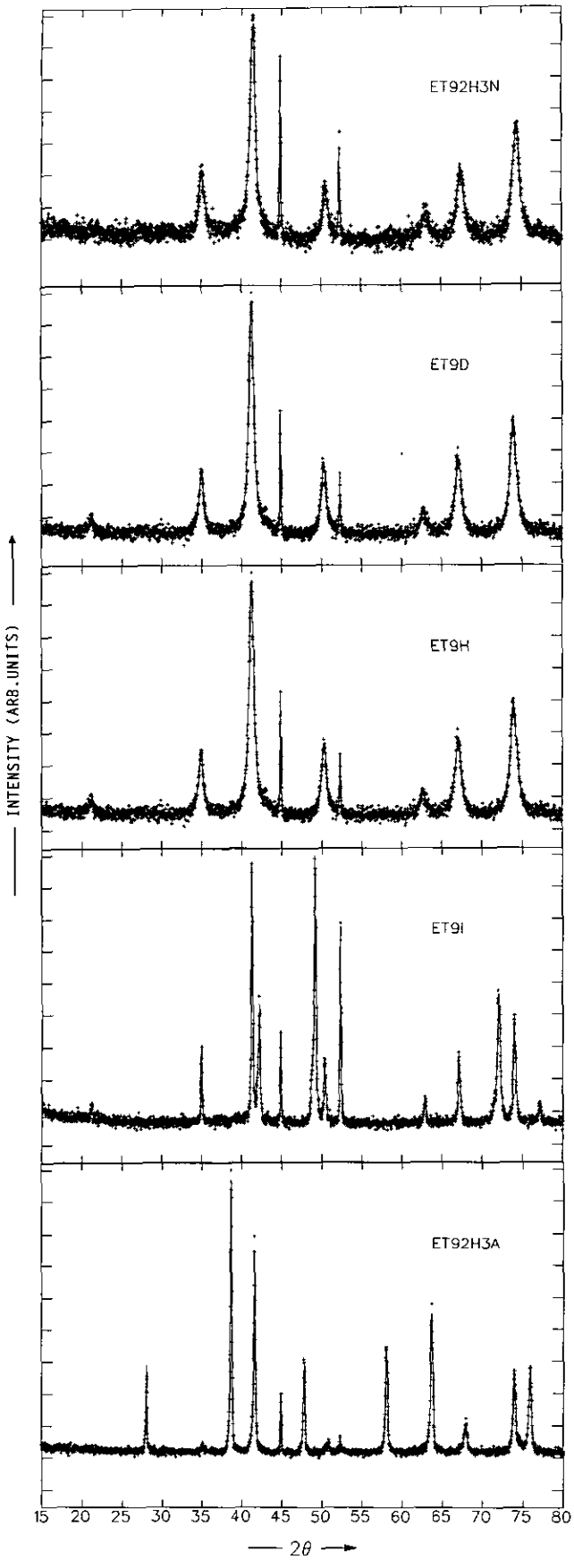

TABLE 2

Cell Parameters and Mean Crystallite Diameters (MCD) along the (311) Lattice Direction as Determined from the X-Ray Diffractograms

	γ-Fe_2O_3		Fe_3O_4		α-Fe_2O_3		
Sample	*a*	MCD	*a*	MCD	*a*	*c*	MCD
ET92H3N	0.8365	14	—	—	—	—	—
ET9D	0.8353	18	—	—	—	—	—
ET9H	—	—	0.8413	15	—	—	—
ET92H3A	—	—	—	—	0.505	1.38	110
ET9I	—	—	0.8403	200	—	—	—

Note. The data for hematite were calculated from the (110) and (104) diffraction lines. All values are given in nm.

agreement between the calculated and experimental line shapes is reasonable. The derived parameters for the high-field component (see Table 3) are in line with those for the A-site subspectrum of magnetite (8), but also with those for both A and B sites of maghemite (9). On the other hand, the average hyperfine field ($\overline{H}_{hf}$) for the second magnetic component is too low to be due to the B-site component of magnetite. Furthermore, its center shift is found to be 0.42 mm/sec and this is again unacceptably low for the B sites in magnetite for which $\delta = 0.66$ mm/s at RT (8). The spectrum at 80 K (Fig. 3b) and the parameters derived from it using the same model as for the RT spectrum closely resemble those for maghemite. However, this is not firm proof for the absence of any magnetite since the spectrum of the latter below T_V is hard to resolve from that of maghemite, especially if the magnetite is present as a minor constituent.

Attempts to fit the RT spectrum of ET92H3N with four discrete Lorentzian-shaped sextets, two for maghemite and two for magnetite, proved unsuccessful. The maghemite subspectra are known to be strongly overlapping with one another and with the A-site component of magnetite. As a consequence, the fitting routine assuming four sextets does not reach convergency, even if restrictions, such as area ratios within each subspectrum fixed at their values as expected from structural considerations, are imposed.

The assignment of the doublet component present in the MS of ET92H3N is not straightforward, mainly because its parameters are rather poorly defined. At RT, the average quadrupole splitting is evaluated to be 1.4 mm/sec, and the corresponding isomer shift is 0.36 mm/

FIG. 2. Powder X-ray diffraction patterns of samples ET92H3N, ET9D, ET9H, ET9I, and ET92H3A. Peaks at 44.8 and 52.3° (2θ) are due to the sample holder. Solid lines represent the fitted patterns.

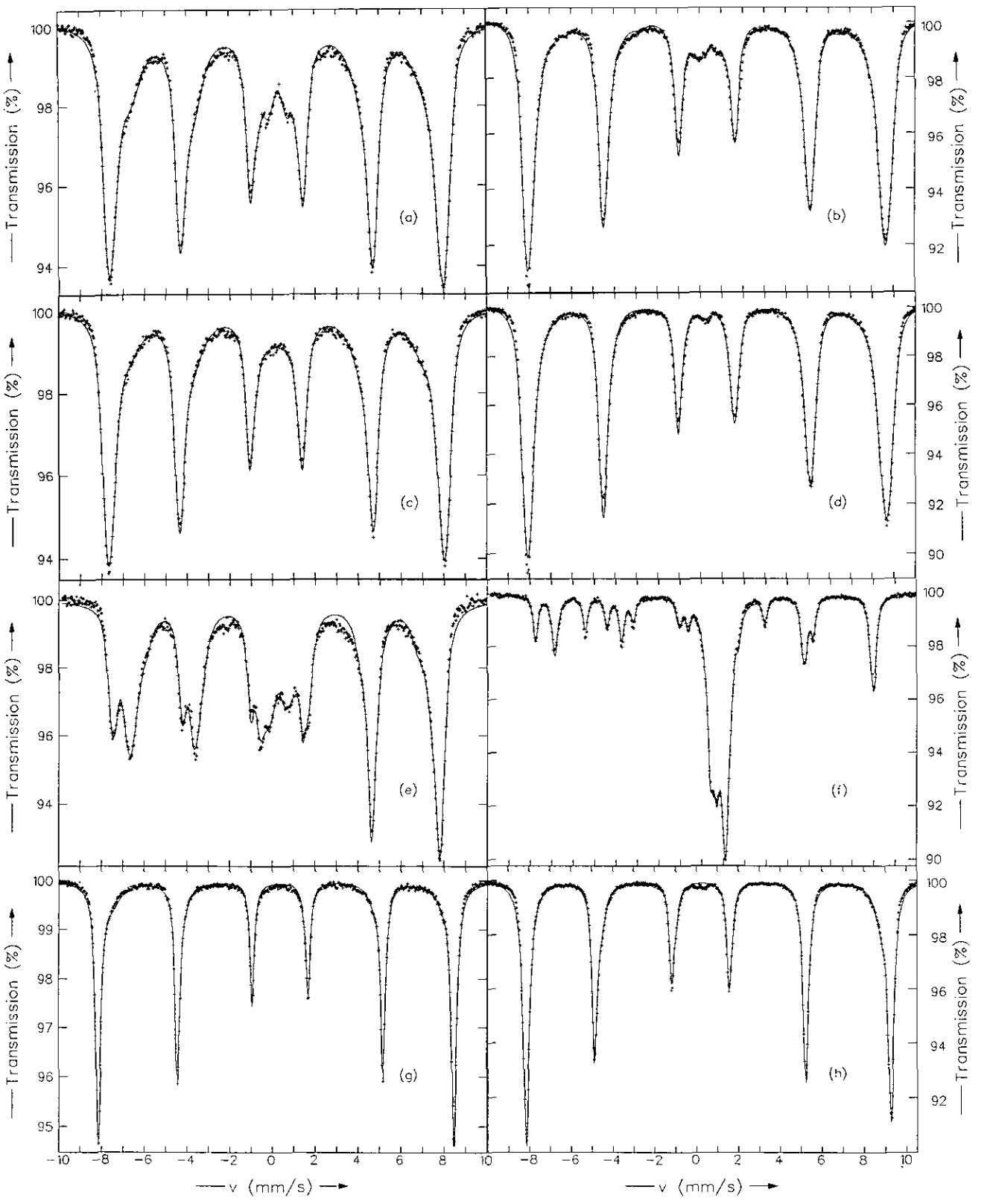

FIG. 3. Mössbauer spectra of the materials obtained from the decomposition of sample ET9 under different conditions: (a) ET92H3N at RT, (b) ET92H3N at 80 K, (c) ET9D at RT, (d) ET9D at 80 K, (e) ET9H at RT, (f) ET9I at RT, (g) ET92H3A at RT, and (h) ET92H3A at 80 K.

sec. This latter value points to a Fe^{3+} state, probably in an octahedral coordination. Both γ-Fe_2O_3 and Fe_3O_4, when present as small-particle systems, may contain a superparamagnetic fraction at RT. This fraction gives rise to a quadrupole doublet with $\Delta E_Q \cong 0.76$ mm/sec (10) in the case of γ-Fe_2O_3 and to two broad singlets centered at $\delta = 0.12$ mm/sec and $\delta = 0.61$ mm/sec, respectively, in the case of Fe_3O_4 (11). Therefore, it is believed that the doublet component is not exclusively due to either maghemite or magnetite, but that it contains a significant contribution from part of the precursor that was not fully transformed in the process. This suggestion is consistent with the observation that after heating ET9 during 4 hr instead of 2 hr, the fractional area *RA* of the doublet at RT has dropped to approximately 5%.

Perhaps more conclusive evidence for the presence of magnetite in ET92H3N was obtained from chemical analysis. Approximately 25 mg of sample was used for each run, and most of the material was dissolved by warm concentrated HCl. The insoluble part proved resistant even to hot HCl, and it was decided to ignore this small fraction in order to avoid oxidation of the Fe^{2+} by air. The ferrous iron was found to be 3.5% (by weight), which corresponds to ≅15% of magnetite. This value is seen as the lower limit, since the procedure is very susceptible to errors due to partial oxidation by air prior to the analysis and also due to the incomplete solubility of the host material.

In conclusion, sample ET92H3N seems to be most likely composed of a mixture of maghemite and magnetite. However, a partial and variable oxidation of the magnetite phase cannot be excluded. Therefore, the two hyperfine-field distributions adjusted to the MS do not have a physical meaning in the sense that they can be associated to two distinct iron species, but rather reflect the presence of a broad distribution of particle sizes and, possibly, of the local composition of the magnetite phase. The broad range of particle dimensions was confirmed by the TEM experiments. Due to clustering of the platelike particles, presumably as a result of interparticle magnetic interactions, the dimensions of the particles could not be determined from the electron micrographs. At this point it is worth mentioning that the RT spectrum of the present sample is very similar to the one ascribed to a mixture of maghemite and Na–maghemite in the paper of Yamanobe *et al.*(4). The broad low-field component was interpreted by these authors as being due to tetrahedral ferric ions in the Na–maghemite structure. However, since no more quantitative details are specified in the paper, it is not possible to further discuss their results in relation to the present ones.

It is well known that small-particle magnetite is readily oxidized to maghemite by heating the material in air at relatively low temperatures (12). Sample ET9D was prepared for that purpose. Its XRD shows only those peaks corresponding to a spinel phase. The cell parameter (see Table 2) is very close to the literature value for cubic maghemite. Further indication for the absence of magnetite was provided by the chemical analysis, which could not detect any Fe^{2+}. The lower limit for the detection of magnetite, under the conditions employed in the present work, is estimated to be 0.2% by weight.

The MS of ET9D (Fig. 3c) at RT has been fitted using the same conditions as for sample ET92H3N. Comparing the shape of these two spectra and also the derived parameter values, it is seen that the major differences concern the relative contributions RA and the δ values for the low-field components. For sample ET9D the center shifts are essentially the same for both distributed sextet components, which is obviously not the case for ET92H3N. Qualitatively, these differences can be explained by the presence of a magnetite contribution in the latter sample, whereas ET9D is an almost pure maghemite phase. Again, it must be stressed that the two magnetic contributions adjusted to the spectrum of ET9D do not represent the A- and B-site components of maghemite, but merely reflect the broad, unresolvable distributions of hyperfine fields for both A and B sites.

As Fig. 3c clearly shows, the overall hyperfine field distribution in ET9D is strongly asymmetric towards the lower field values. This asymmetry gradually diminishes on lowering *T* and at 80 K the individual absorption lines have a more symmetric shape (Fig. 3d). The spectrum is typical for maghemite, the asymmetry in peak depths being due to the superposition of two components with slightly different hyperfine fields and center shifts. The weak central absorption arises from an Fe-containing impurity in the cryostat windows. The line shape asymmetry for small-particle maghemite at higher temperatures has been observed before by several authors (13, 14) and is commonly ascribed to so-called "collective magnetic excitations" which cause the smaller particles to exhibit a lower hyperfine field, the reduction being larger at higher *T*.

Attempts to further improve the crystallinity of sample ET9D proved unsuccessful in that a small amount of hematite was formed (≈5%) when the sample was heated at 400°C during 2 hr without altering the characteristics of the remaining maghemite phase.

As mentioned above, as soon as sample ET92H3N is removed from the furnace, part of the black-grained material (Fe_3O_4) seems to transform to a brownish material which is believed to be maghemite. In order to avoid this rapid oxidation process, another sample was prepared (ET9H) using the same conditions as those applied for ET92H3N, but the material was allowed to cool slowly inside the furnace under N_2 atmosphere in order to prevent oxidation. The XRD pattern of the resulting black

TABLE 3
Mössbauer Parameters of the Products Obtained from Sample ET9

Sample	Temp.	H_{hf}^{b} (kOe)	H_{hf}^{c} (kOe)	N	H_{hf}^{m} (kOe)	$\overline{H}_{hf}$ (kOe)	δ (mm/sec)	$2\varepsilon_Q$[a] (mm/sec)	FWHM (mm/sec)	RA (%)
ET92H3N	RT	450	520	20	486	484	0.32	0	0.39	50
		390	460	20	441	434	0.42	0	1.24	40
	80 K	360	550	50	519	509	0.41	0	0.42	95
ET9D	RT	450	520	20	489	486	0.29	0	0.39	61
		390	460	20	433	432	0.28	0	1.33	32
	80 K	360	550	50	521	513	0.39	0	0.41	99
ET9H		460	510	20	477	476	0.29	0	0.28	23
	RT	360	480	20	443	434	0.58	0	0.52	62
ET9I[+]		—	—	—	489	—	0.26	0	0.24	13
		—	—	—	459	—	0.67	0	0.28	22
		—	—	—	329	—	0.00	0	0.28	11
		—	—	—	—	—	0.98	0.35[b]	0.40	24
		—	—	—	—	—	0.88	0.76[b]	0.39	29
ET92H3A[c]		—	—	—	515	—	0.37	−0.20	0.24	77
	RT	—	—	—	483	—	0.37	0	0.38	23
		—	—	—	540	—	0.48	0.38	0.26	75
	80 K	—	—	—	525	—	0.45	0	0.31	25

Note. H_{hf}^{b} and H_{hf}^{c} are the lower and upper limits for the hyperfine-field distributions; N is the number of divisions of the field range; $2\varepsilon_Q$ is the quadrupole shift; H_{hf}^{m} and $\overline{H}_{hf}$ are the maximum-probability and average hyperfine fields, respectively. FWHM is the full width at half maximum of the elementary sextet patterns constituting the distribution.

[a] Fixed at 0 except for ET92H3A.

[b] These two doublets are ascribed to wustite and the figures refer to the adjusted quadrupole splittings.

[c] Spectra fitted with discrete Lorentzian components.

powder shows only those peaks corresponding to a spinel phase, and the cell parameter is in line with literature values for magnetite. Again, this sample consisted of very small particles with an average size of 15 nm.

The MS of ET9H at RT is reproduced in Fig. 3e. It is consistent with the XRD pattern, indicating that the sample predominantly consists of a magnetite-like phase. When fitted as a superposition of two hyperfine-field distributions and one quadrupole-splitting distribution (full line in the figure), the parameters for the magnetic components were evaluated as indicated in Table 3. The center shifts are close to the values for A- and B-site iron species in stoichiometric magnetite (5), but the average and maximum-probability fields are lower by about 10 kOe. This feature can be explained by the small size of the involved magnetite particles (15). Also, the A- to-B-site area ratio is significantly less than the ideal value 1:2, which is supposedly predominantly due to an artifact of the fitting. Again, the doublet component is poorly defined and its origin therefore could not be traced. Moreover, the fitting model does not provide an excellent reproduction of the experimental line shape. Clearly, one or more additional components are present in the spectrum. A metallic-iron pattern could not be adjusted. The presence of some iron carbides cannot be excluded *a priori*. Such carbides would give rise to Zeeman patterns in the velocity range ±3 mm/sec (16), with a significant doublet contribution at RT.

At 80 K the spectrum of ET9H shows less structure than the RT spectrum. A straightforward and physically meaningful numerical interpretation of the line shape was not found possible. However, it is clear that the visible distinction between the A- and B-site species in the Fe_3O_4 phase has vanished, meaning that the magnetite exhibits a Verwey-like transition. This finding is consistent with the results reported by Topsøe and Mørup (17) for Fe_3O_4 particles with an average size of 10 nm, for which the Verwey transition was found to be around 100 K.

Next, sample ET9I was prepared in an attempt to promote grain growth of the small particles in sample ET9H, but instead a complex mixture of magnetite, metallic iron, and wustite ($Fe_{1-x}O$) was obtained. The XRD pattern clearly shows the presence of these three phases, and the MCD value (200 nm) estimated for the magnetite suggests that the smaller particles of the latter have been transformed into the other two Fe components. The Mössbauer spectrum at RT (see Fig. 3f) has been interpreted straightforwardly as a superposition of two Lorentzian sextets for magnetite, one for metallic iron and two doublets for wustite. The obtained parameters are in excellent agreement with literature values (8, 18).

Finally, well crystallised hematite was obtained by heating sample ET9 at 300°C during 2 hr under O_2 atmosphere. The XRD pattern of sample ET92H3A (Fig. 2) shows, in addition to the sharp peaks corresponding to

α-Fe_2O_3, a weak reflection corresponding to d = 0.298 nm, which is ascribed to maghemite. The crystallinity of the hematite in this sample is much better than that obtained by dehydroxilation of goethite at the same temperature (19). Moreover, the hyperfine fields both at RT and 80 K are very close to the values reported in literature for bulk hematite samples (20). The presence of maghemite could not be avoided, not even by heating sample ET9 at 300°C for 8 hr or at 500°C for 5 min. It is likely, however, that this impurity will be removed by heating for longer periods at this temperature.

Another interesting observation is that heating ET9 for only 5 min at 300°C in O_2 gas flow yields a hematite with the same high degree of crystallinity as compared to the previous one. This finding suggests that the transformation ET9 $\Rightarrow$ α-Fe_2O_3 proceeds in one step, i.e., that maghemite is not formed as an intermediate phase. Further evidence for this one-step transformation is the fact that sample ET9D had to be heated at 400°C during 2 hr in order to produce a minor quantity of hematite.

Finally, it is worth mentioning that literature data for substituted maghemites are scarce and restricted almost entirely to Co, Al, and Ti substitution. Nevertheless, it has never been reported that these substitutional elements can reduce the A- and B-site hyperfine fields to such an extent as reported by Yamanobe *et al.* (4) for Na substitution. As a comparison, typical hyperfine field values for nonsubstituted maghemites at 275K are $H_{hf,A}$ = 506 kOe and $H_{hf,B}$ = 507 kOe. For a 6 at.% Al-substituted maghemite these parameters were found to be 500 and 504 kOe, respectively (9). From these results, which were obtained from applied-field Mössbauer spectroscopy, it can be concluded that both hyperfine fields have equal magnitude and that the Al substitution has only a minor effect on these values. Nonstoichiometry would probably not cause such a high decrease in the hyperfine fields either, since a slight increase is observed in going from magnetite to maghemite (21). The lack of systematic Mössbauer studies on Na–maghemites, supported by experiments from relevant complimentary techniques, combined with the rather poor statistical quality of the currently available spectral data, implies that the interpretation and conclusions of Yamanobo *et al.* are at best to be regarded with some reserve.

CONCLUSION

A sol-gel method has been successfully applied for the preparation of three different iron oxides, namely hematite, maghemite, and magnetite. Although the latter two are poorly crystallized, bulk hematite was easily obtained at relatively low temperatures. The spinel oxides show a very broad size distribution with an average particle size of about 15 nm. Under certain conditions a mixture of small-particle maghemite and magnetite was obtained. The shape of its Mössbauer spectrum at RT, as well as the average hyperfine fields derived from it, was found to be very similar to those ascribed to sodium–maghemite by Yamanobe *et al.* (4), although no sodium was involved in the preparation of the present samples.

ACKNOWLEDGMENTS

This work was supported in part by the Fund for Joint Basic Research (Belgium, Grant 2.0014.93) and by Conselho Nac. de Des. Cient. e Tecnológico (Brazil).

REFERENCES

1. U. Schwertmann and R. M. Cornell, "Iron Oxides in the Laboratory: Preparation and Characterisation." VCH, New York, 1991.
2. B. Gillot and A. Rousset, *Phys. Status Solidi A* **118,** K5 (1990).
3. N. Takahashi, N. Kakuda, A. Ueno, K. Yamaguchi, and T. Fujii, *Jpn. J. Appl. Phys.* **28,** 244 (1989).
4. Y. Yamanobe, K. Yamaguchi, K. Matsumoto, and T. Fujii, *Jpn. J. Appl. Phys.* **30,** 478 (1991).
5. R. E. Vandenberghe and E. De Grave, *in* "Mossbauer Spectroscopy Applied to Inorganic Chemistry" (G. J. Long and F. Grandjean, Eds.), Vol. 3, p. 59. Plenum, New York, 1989.
6. H. P. Klug and L. E. Alexander, "X-Ray Diffraction Procedures for Polycrystalline and Amorphous Materials," p. 687. Wiley, New York, 1974.
7. E. De Grave and A. Van Alboom, *Phys. Chem. Minerals* **18,** 337 (1991).
8. E. De Grave, R. M. Persoons, R. E. Vandenberghe, and P. M. A. de Bakker, *Phys. Rev. B* **47,** 5881 (1993).
9. G. M. da Costa, E. De Grave, R. E. Vandenberghe, L. H. Bowen, and P. M. A. de Bakker, *Clays Clay Miner.*, in press.
10. P. M. A. de Bakker, E. De Grave, R. E. Vandenberghe, L. H. Bowen, R. J. Pollard, and R. M. Persoons, *Phys. Chem. Minerals* **18,** 131 (1991).
11. S. Mørup and H. Topsøe, *J. Magn. Magn. Mater.* **31,** 953 (1983).
12. T. Elder, *J. Appl. Phys.* **36,** 1012 (1965).
13. E. Tronc, J. P. Jolivet, and J. Livage, *Hyperfine Interact.* **54,** 737 (1990).
14. A. H. Morrish and K. Haneda, *J. Magn. Magn. Mater.* **35,** 105 (1983).
15. S. Mørup and H. Topsøe, *Appl. Phys.* **11,** 63 (1976).
16. E. Lox, G. B. Marin, E. De Grave, and P. Bussière, *Appl. Catal.* **40,** 197 (1988).
17. H. Topsøe and S. Mørup, in "Proceedings, International Conference on Mössbauer Spectroscopy, Cracow, Poland, 1975" (A. Z. Hrynkiewicz and J. A. Sawicki, Eds.), Vol. 1, p. 321. Akademia Gorniczo-Hutnicza, Cracow.
18. E. Murad and H. Johnston, "Mössbauer Spectroscopy Applied to Inorganic Chemistry" (G. J. Long, Ed.), Vol. 2, p. 507. Plenum, New York, 1987.
19. G. M. da Costa and M. F. de Jesus Filho, *J. Mater. Sci.* **27,** 6116 (1992).
20. E. Murad, "Iron in Soils and Clay Minerals" (J. W. Stucki, B. A. Goodman, and U. Schwertmann, Eds.), p. 309. Reidel, Dordrecht, 1985.
21. H. Annersten and S. Hafner, *Z. Kristallogr.* **137,** 321 (1973).